



Research paper

Circuit Analog Absorber Based on a Double-Layer of Resistor-Loaded Strip Arrays with Various Bandwidths according to Selecting the Polarization

S. Barzegar-Parizi*

Department of Electrical Engineering, Sirjan University of Technology, Sirjan, Iran.

Article Info

Article History:

Received 03 September 2024
Reviewed 17 November 2024
Revised 12 December 2024
Accepted 15 December 2024

Keywords:

Resistor-loaded strips
Microwave absorber
Circuit model
TM
TE
FSS
Reflectivity

*Corresponding Author's Email
Address:
barzegarparizi@sirjantech.ac.ir

Abstract

Background and Objectives: The design of the circuit analog absorbers including resistive and conductive patterns on a dielectric substrate placed above the ground plane with a free spacer is interesting for researchers in the microwave regime. Broad absorption band can be achieved by appropriately designing the structure parameters that lead to matching the input impedance of the structure with the impedance of free space over a wide operating band. In this study, a wideband circuit analogue absorber including double-layer of resistive frequency selective surfaces (FSS) is proposed.

Methods: The proposed structure is composed of two layers of periodic arrays of strips loaded with lumped resistors deposited on dielectric substrates and separated by an air spacer. Strips of each layer are orthogonal to each other. The structure is placed on a metallic back reflector with an air spacer. The bottom resistive FSS including resistor-loaded strips directed in the x-direction plays the effective role of producing the resonant frequencies with exciting TM polarization waves and leads to a wide high-frequency absorption band, while the top resistive FSS, including resistor-loaded strips directed in the y-direction plays the effective role in exciting the resonances for TE polarization that can produce a broad low frequency absorption band. Indeed, in each polarization, one of the resistive FSS acts as a resonator while the other resistive FSS acts as a transparent layer and transmits the wave. A circuit model for characterizing the proposed structure is presented for both TE and TM polarizations in the subwavelength regime, which shows good agreement with the full-wave simulations.

Results: The results demonstrate that the reflectivity below -10 dB (absorption above 90%) obtains from 3.55 to 9.82 GHz (fractional bandwidth of 93%) under normal incidence for TE polarization while with TM incident wave excitation, the absorption above 90% from 9.44 to 20.85 GHz (fractional bandwidth of 75%) can be achieved.

Conclusion: The proposed structure leads to a wideband absorber with various bandwidths corresponding to exciting TE and TM incident waves. Most of the proposed structures in the literature produce similar bandwidths for both polarizations. Therefore, a polarization-controlled wideband absorber is designed in this task.

This work is distributed under the CC BY license (<http://creativecommons.org/licenses/by/4.0/>)



Introduction

Electromagnetic absorbers have found many potential applications in different systems. The wide bandwidth over the operating band, and smaller thickness are the essential parameters, in the design of microwave

absorbers. A resistive sheet placed a quarter-wavelength distance above the conducting plate [1]-[2] known as the Salisbury screen, was presented decades ago to reduce the reflection and result in absorbing the incident electromagnetic wave. Despite its structural simplicity,

due to the conforming of quarter-wavelength conditions at a single specified frequency, the absorption bandwidth of the Salisbury screen was relatively narrow. Jaumann absorber utilizing additional resistive layers and spacers was introduced [3]-[4] to improve the bandwidth of the Salisbury screen. However, increasing the resistive layers and spacers enhances the total thickness and it limits its scope of application. The circuit analog (CA) absorbers were proposed for achieving electromagnetic absorbers with wide bandwidth and small thickness [5]-[30]. The circuit analog absorbers are made by depositing conductive/resistive patterns or resistor-loaded patterns on a dielectric layer placed above a metallic back reflector with a free spacer. By appropriately designing the structure parameters and choosing the chip resistors, the input impedance of the structure could be matched with free space impedance over a wide operating band, and the broad absorption band occurs.

In [5]-[9], the structures based on the conductive patterns and dielectric layers have been proposed to achieve the narrow and wide absorption bands. For example, in [6], a single layer of copper FSS as swastika-like patterns has been employed to design a narrow band absorber. The multilayered structures of metallic loops and closed ring resonators have been proposed in [7] and [8], respectively, for achieving broadband and dual-band absorbers. In [9], a multilayered structure of crossed dipoles has been proposed to realize triple absorption bands. In [10]-[14], the frequency selective surfaces including resistive patterns are employed to realize the broad absorption bands. The resistive treble-square loops, resistive crisscross and fractal square patches and resistive quadruple hexagonal loops have been respectively utilized to realize broadband absorbers in [11], [12], and [13]. In [15]-[30], resistor-loaded patterns have been applied to achieve broadband absorbers. In [16] and [21]-[22], broadband absorbers based on square loops loaded by lumped-resistors have been presented. Lumped resistor loaded double octagonal rings have been employed to realize wideband absorber in [17]. In [23], a single layer of a modified circular ring and in [24], a single layer of double patterns of rectangular and ring split ring resonators loaded by lumped resistors have been applied to achieve wideband absorbers. In recent tasks, the researchers have designed absorbers consisting of multiple vertically stacked FSS layers to increase the bandwidth. In [28], a structure using a dual layer of resistor-loaded metallic strips has been proposed to achieve a wide absorption band for both TE and TM modes. The structure includes the lossy layer consisting of two orthogonal layers of dual-resistor-loaded metallic strips printed on both sides of a dielectric substrate. In [29], a polarization-insensitive wideband absorber has been proposed based on a multi-layer of square loops loaded with lumped resistors printed on the

dielectric layers separated by an air spacer. In this task, the bottom resistive surface in combination with the top resistive surface, enhances the bandwidth by creating another resonance. A polarization-insensitive circuit analog absorber containing two lossy layers of a single square-loop and double-square-loop loaded with lumped resistors has been designed in [30] to obtain an ultra-wide absorption band. All of these aforementioned absorber designs are polarization-insensitive and capable of absorbing waves for both polarizations in the same absorption band. Therefore, the design of an absorber with selectivity bandwidth according to the polarization is interesting. In [31]-[34], the polarization-controlled structures that display the various absorption bands according to the selection of the polarization have been presented. However, the proposed structures present narrow absorption bands with exciting TE and TM incident waves.

In this paper, a wideband absorber is designed with various bandwidth range according to exciting each polarization. The proposed structure is composed of double layers of resistor-loaded metallic strips array printed on a dielectric substrate. The strips of one layer are orthogonal to the other layer. Two layers are separated by an air spacer, and then the bottom layer is placed above a metallic film with another air spacer. The various wide absorption bands can be achieved with the selection of polarization. The strips of the top resistive layer are arranged in y-direction while the strips of the bottom resistive layer are arranged in x-directions. Therefore, by properly designing the geometrical parameters and choosing the chip resistors of the structure, the structure can absorb the incident waves for TE polarization at low frequencies between ranges of 3.55 to 9.82 GHz, while it can absorb the incident waves for TM polarization at higher frequency between ranges of 9.44 to 20.85 GHz. An equivalent circuit model is introduced for both polarizations. Therefore, by changing the polarization, the absorption bandwidth would change. The following paper is organized as follow: the structure and analysis are presented in section 2. The proposed structure leads to various absorption bands with exciting TE and TM incident waves. The equivalent circuit model is presented for both polarizations. It's demonstrated that the top resistive layer plays the resonator role modeled as two series R-L-C branches by exciting TE mode while the situation is vice versa for TM mode. For TM polarization, the bottom resistive layer is modeled as two series R-L-C branches. Finally, Section 3 presents the main conclusions.

Structure and Design

A single unit cell of the proposed structure, which comprises two resistive frequency selective surfaces printed on dielectric layers is displayed in Fig. 1. The thickness of dielectric spacers is defined as h_{d1} and h_{d2} .

These layers are separated by an air spacer with a thickness of h_{s1} and h_{s2} . The overall structure has been terminated by a metal film acting as a back reflector.

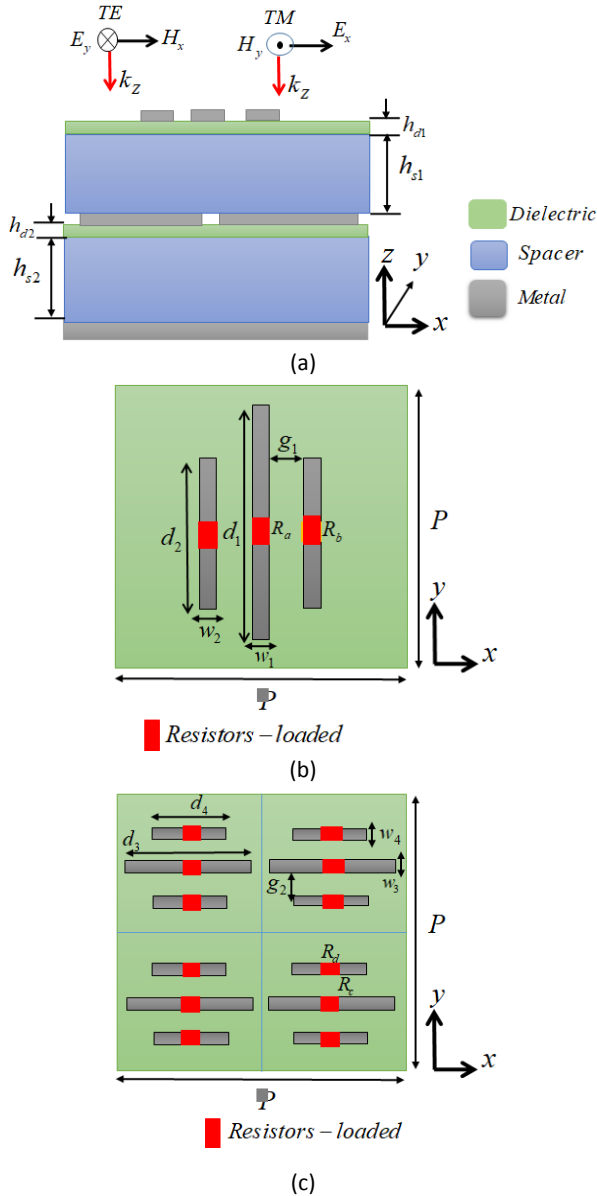


Fig. 1: (a) Perspective view of the structure including a double layer of the resistive frequency selective surfaces deposited on a dielectric substrate placed on a spacer and a metallic reflector at the bottom. (b) Top view of the top resistive FSS including three resistor-loaded strips directed in y -direction (c) Top view of the bottom resistive FSS including four cells of three resistor-loaded strips directed in x -direction.

The unit cell of the top resistive frequency selective surface (TRFSS) is built of three resistor-loaded strips directed in the y -direction. The length and width of the central strip is d_1, w_1 and two neighbor strips with the length and width of d_2, w_2 are placed at the right and the left of the central strip with space of g_1 . Lumped resistors are placed at the center of each strip with values of R_a and R_b . The bottom resistive frequency selective surface (BRFSS) is composed of four sub unit cells of three

resistor-loaded strips directed in x -direction. The length and width of the central strip is d_3, w_3 , and two neighbor strips with the length and width of d_4, w_4 are placed at the right and the left of the central strip with space of g_2 . Lumped resistors are placed at the center of each strip with values of R_c and R_d . RT/Duroid5880 with a relative permittivity of 2.2 has been used as dielectric. Copper with conductivity $\sigma = 5.8 \times 10^7$ S/m and a thickness of 0.02 mm is considered for the metal strips and the bottom metallic film. The period of the structure is supposed to be P in x - and y -directions.

Table 1: Detailed unit cell parameters of the proposed structure

Description of Parameter	Symbol	Value
Period length	P	26 mm
Thickness of top dielectric layer	h_{d1}	0.45 mm
Thickness of bottom dielectric layer	h_{d2}	0.2 mm
Thickness of top free spacer	h_{s1}	5 mm
Thickness of bottom free spacer	h_{s2}	5 mm
Central strip length of the TRFSS	d_1	25mm
Central strip width of the TRFSS	w_1	0.5 mm
smaller strip length of the TRFSS	d_2	15 mm
smaller strip width of the TRFSS	w_2	0.5 mm
Central strip length of the BRFSS	d_3	11 mm
Central strip width of the BRFSS	w_3	0.4 mm
smaller strip length of the BRFSS	d_4	5 mm
smaller strip width of the BRFSS	w_4	0.4 mm
gap between strips of the TRFSS	g_1	3.5 mm
gap between strips of the BRFSS	g_2	1.5 mm
Lumped resistor at the center of longer strips of the TRFSS	R_a	125 Ω
Lumped resistor at the center of smaller strips of the TRFSS	R_b	100 Ω
Lumped resistor at the center of longer strips of the BRFSS	R_c	75 Ω
Lumped resistor at the center of smaller strips of the BRFSS	R_d	50 Ω

The proposed structure leads to wideband absorption bands by exciting TE and TM incident waves. By exciting the TE incident wave where the electric field is in the y -direction and the magnetic field is in the x -direction, the top resistive frequency selective surface plays an essential role in exciting the resonant frequencies. It leads to a low-frequency wide absorption band. In this case, the bottom resistive FSS acts as a transparent layer and transmits the wave. At the same time, a high-frequency absorption band can be achieved by exciting TM incident waves. In this case, the bottom frequency selective surface plays an essential role in exciting the resonant frequencies, and the top resistive FSS transmits the wave. In Table. 1, the

parameters of a single unit cell of the proposed structure are presented. Fig. 2(a) and (b) show the simulated reflectivity and absorption of the proposed absorber under the normal incidence for TE polarization. The simulated results display the reflectivity below -10 dB (equal to absorption above 90%) from 3.55 to 9.82 GHz with a fractional bandwidth of 93%. Fig. 2(c) and (d) demonstrate the simulated reflectivity and absorption of the resistive absorber under the normal incidence for TM polarization. The simulated results show that the reflectivity below -10 dB (equal to absorption above 90%) occurs from 9.44 to 20.85 GHz with fractional bandwidth of 75%.

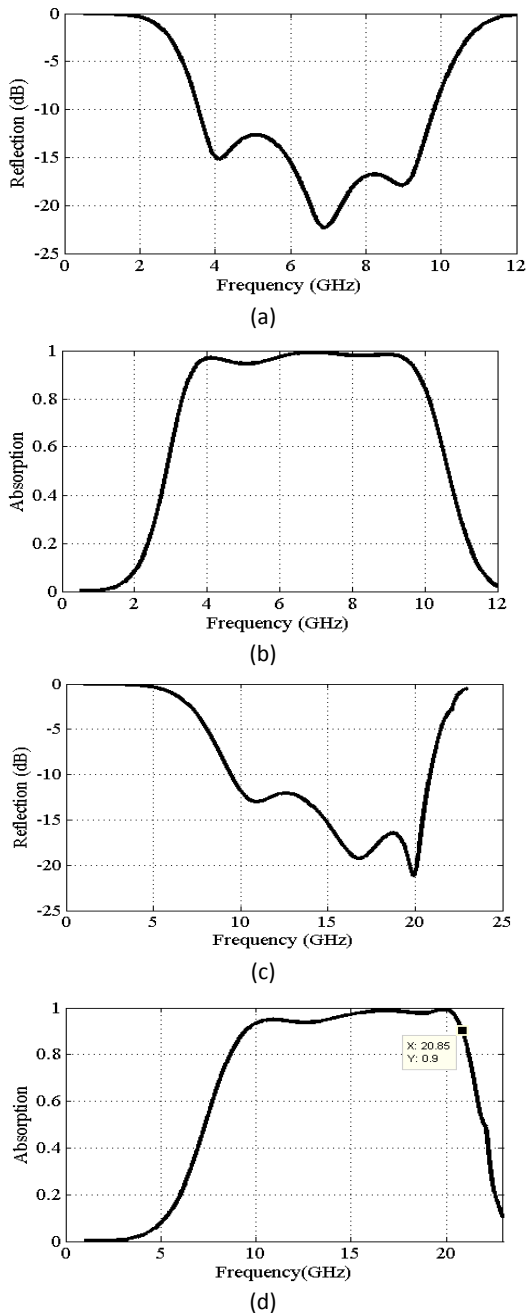


Fig. 2: Simulated (a) reflectivity (b) absorption spectra of the structure of Fig.1 for TE polarization (c) reflectivity (d) absorption spectra for TM polarization.

In Fig. 3, the variations of the lumped resistors loaded on strips are surveyed on the absorption spectra. Fig. 3(a) shows the absorption spectra of the proposed structure for TE polarization, when the lumped resistors of the top resistive layer are varied. As observed, with the selection of $R_a=100\ \Omega$, $R_b=75\ \Omega$ and values more than them, high absorption can be achieved. The variations of the lumped resistors of the bottom resistive layer on absorption spectra for TM polarization are demonstrated in Fig. 3(b).

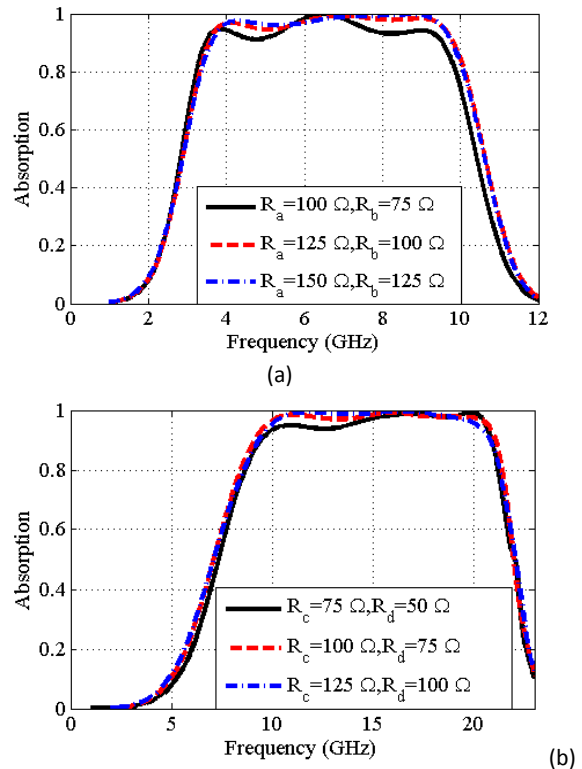


Fig. 3: Simulated absorption spectra of the structure with various lumped resistors (a) for TE polarization (b) for TM polarization.

Furthermore, to better understand the absorber behavior, the equivalent circuit models are presented for both TE and TM modes in the subwavelength regime. The circuit model corresponding to the proposed absorber is illustrated in Fig. 4(a) for the TE polarization wave and (b) for the TM polarization wave, respectively. In the TE case, the top frequency selective surface plays an essential role in exciting the resonant frequencies modeled as two branches of series resistor-inductor-capacitor (RLC) circuits connected in parallel. R_1 , L_1 , and C_1 show the resistance, inductance, and capacitance corresponding to the central metallic strip, respectively, while R_2 , L_2 , and C_2 represent those of smaller metallic strips. The values of the lumped elements corresponding to the resistor-loaded strips of top frequency selective surfaces for TE polarization are defined as: $C_1=0.06\ \text{pF}$, $L_1=19\ \text{nH}$, $R_1=230\ \Omega$, $C_2=0.027\ \text{pF}$, $L_2=16.5\ \text{nH}$ and $R_2=300\ \Omega$. In this case, the bottom resistive FSS of the resistor-loaded strips acts as a transparent layer and transmits the wave. In TM case, the situation is vice versa. In this case, the

bottom frequency selective surface plays an essential role in exciting the resonant frequencies which are modeled as two branches of series resistor-inductor-capacitor (RLC) circuits connected in parallel. R_3 , L_3 , and C_3 show the resistance, inductance, and capacitance equivalent to the central metallic strip, respectively, while R_4 , L_4 , and C_4 specify those of smaller metallic strips. The values of the lumped elements [21] corresponding to the resistor-loaded strips of the bottom frequency selective surfaces for TM polarization are defined as: $C_3=0.02$ pF, $L_3=10.5$ nH, $R_3 = 230\Omega$, $C_4=0.008$ pF, $L_4=9.7$ nH and $R_4 = 300\Omega$. In this case, the top resistive FSS of the resistor-loaded strips acts as a transparent layer and transmits the wave. To demonstrate the role of the top resistive FSS as a transparent layer for TM polarization, the S-parameters of a single layer of top resistive FSS are plotted in Fig. 5 for TM polarization. Two ports are considered at the top and bottom of this layer for computing the S-parameters. The transmission and reflection coefficients are plotted in Fig. 5. As observed, this layer transmits the waves for TM polarization (S_{12} is 0 dB) and acts as a transparent layer.

The dielectric layers are modelled by the transmission lines of the characteristic admittance of $Y_d = \sqrt{\epsilon_r} Y_0$ and the propagation constant of $\beta_d = \beta_0 \sqrt{\epsilon_r}$ with lengths of h_{d1} and h_{d2} . The air spacers are modelled by the transmission lines of the characteristic admittance of Y_0 and the propagation constant of β_0 with lengths h_{s1} and h_{s2} . The bottom metallic film is modelled by the short circuit in the equivalent circuit model.

In TE case, the input admittance of the structure is computed as:

$$Y_{in} = Y_{sur,1} + Y_{sur,2} + Y_{slab}, \quad (1)$$

$$Y_{sur,i} = \frac{1}{R_i + j(\omega L_i - \frac{1}{\omega C_i})}, \quad (i=1,2) \quad (2)$$

$$Y_{slab1} = j \frac{Y_d (Y_d \tan(\beta_d h_{d2}) - Y_0 \cot(\beta_0 h_{s2}))}{Y_d + Y_0 \cot(\beta_0 h_{s2}) \tan(\beta_d h_{d2})} \quad (3)$$

$$Y_{slab2} = Y_0 \frac{(Y_{slab1} + jY_0 \tan(\beta_0 h_{s1}))}{Y_0 + jY_{slab1} \tan(\beta_0 h_{s1})} \quad (4)$$

$$Y_{slab} = Y_d \frac{(Y_{slab2} + jY_d \tan(\beta_d h_{d1}))}{Y_d + jY_{slab2} \tan(\beta_d h_{d1})} \quad (5)$$

where $Y_{sur,i}$ ($i=1,2$) is the admittance of the strips loaded with lumped resistors and Y_{slab} is the equivalent admittances of the conductor-backed dielectric slabs and air spacers.

Finally, the values of the absorption can be computed as:

$$A(\omega) = 1 - R(\omega) = 1 - \left| \frac{(Z_{in}/Z_0) - 1}{(Z_{in}/Z_0) + 1} \right|^2 \quad (6)$$

In which, $Z_{in} = Y_{in}^{-1}$ and Z_0 is the free-space impedance. When the impedance matching conditions over a specified frequency range occur, the maximum absorption can be obtained on this frequency range.

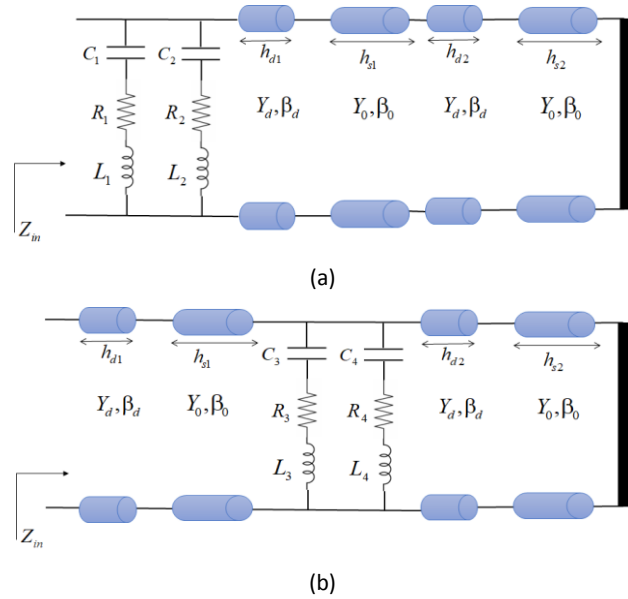


Fig. 4: The equivalent circuit model of the proposed structure for (a) TE and (b) TM polarizations in subwavelength regime.

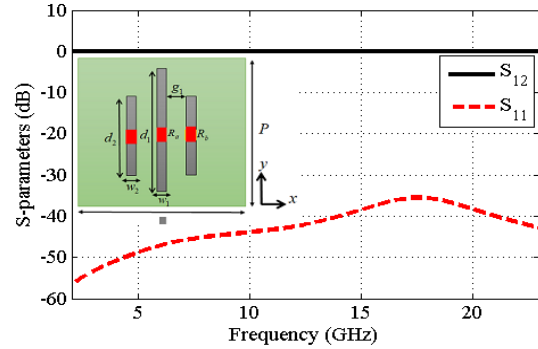


Fig. 5: The S-parameters of a single layer of top resistive FSS for TM polarization.

The comparison between the result extracted by the circuit model analysis and the results obtained by HFSS simulations are displayed in Fig. 6(a) for the proposed structure with parameters presented in Fig. 2 for TE polarization. As demonstrated, the result obtained by the circuit model is in good agreement with the full-wave simulation results.

In the TM case, the input admittance is computed as:

$$Y_{in} = Y_d \frac{(Y_{slab4} + jY_d \tan(\beta_d h_{d1}))}{Y_d + jY_{slab4} \tan(\beta_d h_{d1})} \quad (7)$$

$$Y_{slab4} = Y_0 \frac{(Y_{slab3} + jY_0 \tan(\beta_0 h_{s1}))}{Y_0 + jY_{slab3} \tan(\beta_0 h_{s1})} \quad (8)$$

$$Y_{slab3} = Y_{sur,3} + Y_{sur,4} + Y_{slab1}, \quad (9)$$

$$Y_{sur,i} = \frac{1}{R_i + j(\omega L_i - \frac{1}{\omega C_i})}, (i = 3, 4) \quad (10)$$

The result extracted by the circuit model is compared to the HFSS simulation result for TM polarization in Fig. 6(b).

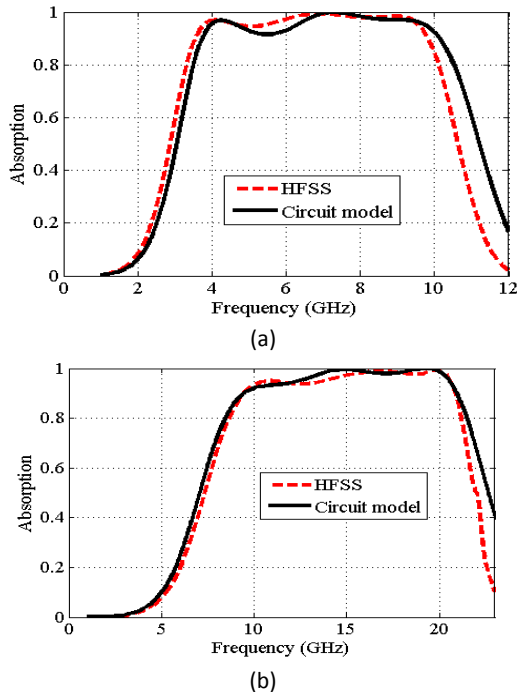


Fig. 6: the results extracted by the circuit model are compared to the HFSS simulations for the proposed structure for (a) TE polarization (b) TM polarization.

However, it is clear that without each of the resistive layers and its underlying dielectric, the absorption occurs for one of the polarizations. For example, if one puts up the top resistive layer and its underlying dielectric above the metallic film with an air spacer of thickness of $h_{s1} + h_{s2} = 10 \text{ mm}$, the new structure absorbs the incident waves for just TE polarization. Suppose the bottom resistive layer and its underlying dielectric have been placed above the metallic film with an air spacer of thickness of $h_{s2} = 5 \text{ mm}$. In that case, the structure absorbs the incident waves for just TM polarization. Fig. 7 shows the absorption spectra for structures without one of the resistive FSS for TE and TM polarizations.

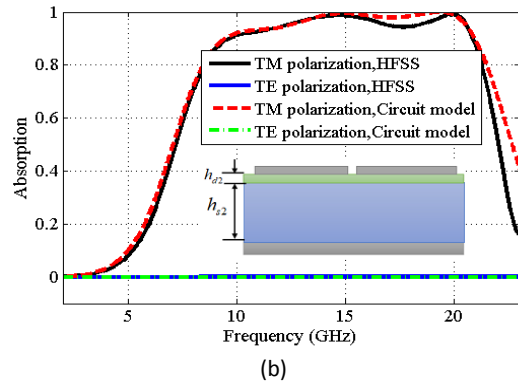
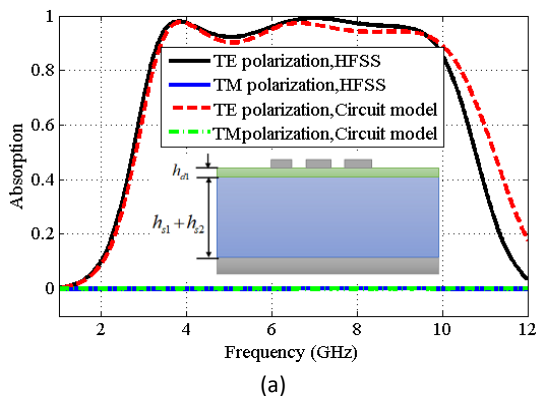


Fig.7: Simulated absorption spectra of the structure without considering (a) the bottom resistive layer and its underlying dielectric (b) the top resistive layer and its underlying dielectric and top air spacer under the normal incidence.

In the following, the performance of the structure with respect to the incident angle is investigated. As mentioned, the performance depends on polarization. For each polarization, the structure leads to a specified absorption spectra. Here, the structure's performance concerning the angle of incidence for each polarization is evaluated. Fig. 8 illustrates the absorption spectra as a function of the frequency and the incident angle up to 50° for TE and TM polarizations, respectively. For both TE and TM polarizations, absorption above 80% can be achieved for the incident angles up to 30° . For TE polarization, the bandwidth decrease with increasing the angle of incidence. For TM polarization, the absorption values are reduced in the middle of the bandwidth.

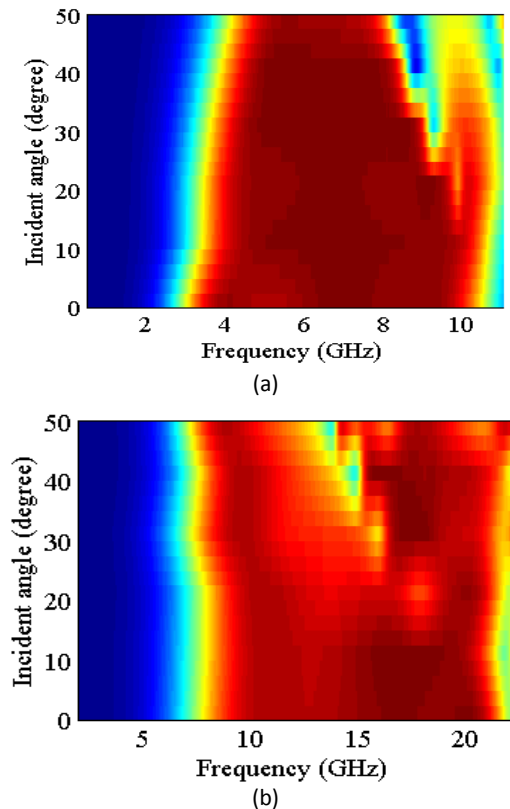


Fig. 8 The Absorption spectra of the proposed structure as a function of different incident angles of (a) TE polarization, and (b) TM polarization.

Finally, comparisons between the designed absorber and the other absorbers are performed in the Table 2. The comparisons are performed in terms of structure and performance. As observed, the structures proposed in [28]-[30] are symmetric and produce a wide absorption band for both TE and TM polarizations. In the present task, the proposed structure causes the absorption performance depending on the polarization. The proposed structure leads to various bandwidths with exciting polarization. Although, the structures proposed in [31]-[34] present the polarization-controlled absorbers. However, the proposed structures are narrowband absorbers, while this task presents a wideband absorber.

Table 2: Performance comparison of proposed absorber to other task

Ref	Structure	Polarization-controlled absorber	Performance
[28]	Two layers of resistor-loaded metallic strips	No	wideband for both TE and TM (3-14 GHz)
[29]	Two layers of square loops loaded with lumped resistors	No	wideband for both TE and TM (4.96 to 18.22 GHz)
[30]	Two layers of square loops loaded with lumped resistors	No	Wideband for both TE and TM (1.92 to 16.87 GHz)
[31]	A metallic FSS of a circular enclosure containing T-shaped resonator	Yes	Quad narrow bands at 9.948, 13.26, 14.92, and 15.80 GHz for TE
[32]	A metallic FSS of split-ring resonators	Yes	Triple narrow bands at 2.4, 5.2 and 5.8, GHz for TE/ Quad-bands at 4.6, 5.3, 6.5, and 6.8 GHz
[33]	A set of wires etched as Yagi-Uda shaped FSS	Yes	A single narrow band at 6.64 GHz for TM / penta-bands at 11.68, 13.58, 15.48, 17.38, and 19.28 GHz for TE
[34]	Yagi-Uda shaped FSS	Yes	Triple narrow bands at 10.64, 12.08, 14.92, and 14.09 GHz for TE
This work	Two layers of resistor-loaded strips	Yes	Wideband from 3.55 to 9.82 GHz for TE/ Wideband from 9.44 to 20.85 GHz for TM

Conclusion

In this paper, a wideband absorber with various bandwidths associated with exciting TE and TM incident waves has been designed. The proposed structure is composed of two stacked resistive layers printed on a dielectric substrate. A single unit cell of the top resistive layer includes three resistor-loaded strips directed in the y-direction that lead to excite the resonances for TE

polarization. In contrast, the bottom resistive layer is composed of four unit cells of three resistor-loaded-strips in the x-direction that leads to excite the resonances for TM polarization. In each polarization, other resistive layer transmitted the wave. The structure led to absorption above 90% from 3.55 to 9.82 GHz for TE polarization, while with TM incident wave excitation, the absorption above 90% from 9.44 to 20.85 GHz has been achieved. Hence, in this task, a polarization-controlled wideband circuit analog absorber has been proposed.

Author Contributions

S. Barzegar-Parizi designed and analyzed the structure. She interpreted the results and wrote the manuscript.

Acknowledgment

This work is completely self-supporting, thereby no any financial agency's role is available.

Conflict of Interest

The author declare no potential conflict of interest regarding the publication of this work. In addition, the ethical issues including plagiarism, informed consent, misconduct, data fabrication and, or falsification, double publication and, or submission, and redundancy have been completely witnessed by the author.

Abbreviations

FSS	Frequency Selective Surface
TE	Transverse Electric
TM	Transverse Magnetic
CA	Circuit Analog
TRFSS	Top Resistive Frequency Selective Surface
BRFSS	Bottom Resistive Frequency Selective Surface

References

- [1] W. W. Salisbury, "Absorbent body of electromagnetic waves," US Patent 2599944, 1952.
- [2] R. L. Fante, M. T. McCormack, "Reflection properties of the Salisbury screen," *IEEE Trans. Antennas Propag.*, 36(10): 1443-1454, 1988.
- [3] L. J. Du Toit, "design of jauman absorbers," *IEEE Trans. Antennas Propag. Magazin*, 36(6): 17-25, 1994.
- [4] E. F. Knott, J. F. Shaeffer, M. T. Tuley, "Radar cross section," SciTech, Raleigh, NC, USA, 2nd ed., 2004.
- [5] T. S. Pham, H. Zheng, L. Chen, B. X. Khuyen, Y. Lee, "Wide-incident-angle, polarization-independent broadband-absorption metastructure without external resistive elements by using a trapezoidal structure," *Sci. Rep.*, 14: 10198, 2024.
- [6] S. Ghosh, S. Bhattacharyya, K. V. Srivastava, "Bandwidth-enhanced of an ultra-thin polarization insensitive metamaterial absorber," *Microw. Opt. Technol. Lett.*, 56(2): 350-355, 2014.
- [7] H. Xiong, et al., "An ultrathin and broadband metamaterial absorber using multi-layer structures," *J. Appl. Phys.*, 114: 064109, 2013.
- [8] S. Bhattacharyya, S. Ghosh, D. Chaurasiya, et al., "Bandwidth-enhanced dual-band dual-layer polarization-independent ultra-thin metamaterial absorber," *Appl. Phys. A*, 118: 207-215, 2015.

- [9] S. Ghosh, S. Bhattacharyya, D. Chaurasiya, et al., "Polarization-insensitive and wide-angle multilayer metamaterial absorber with variable bandwidths," *Electron. Lett.*, 51(14): 1050-1052, 2015.
- [10] F. Costa, et al., "Analysis and design of ultrathin electromagnetic absorbers comprising resistively loaded high impedance surfaces," *IEEE Trans. Antennas Propag.*, 58(5): 1551-1558, 2010.
- [11] M. Li, et al., "An ultrathin and broadband radar absorber using resistive FSS," *IEEE Antennas Wirel. Propag. Lett.*, 11: 748-751, 2012.
- [12] L. K. Sun, H. F. Cheng, Y. J. Zhou, et al., "Broadband metamaterial absorber based on coupling resistive frequency selective surface," *Opt. Exp.*, 20(4): 4675-4680, 2012.
- [13] S. N. Zabri, R. Cahill, A. Schuchinsky, "Compact FSS absorber design using resistively loaded quadruple hexagonal loops for bandwidth enhancement," *Electron. Lett.*, 51(2): 162-164, 2015.
- [14] P. C. Zhang, et al., "A wideband wide-angle polarization-insensitive metamaterial absorber," in *Proc. Progress in Electromagnetics Research Symp.*, Guangzhou, China, 941-943, 2014.
- [15] M. Yoo, S. Lim, "Polarization-independent and ultrawideband metamaterial absorber using a hexagonal artificial impedance surface and a resistor-capacitor layer," *IEEE Trans. Antennas Propag.*, 62(5): 2652-2658, 2014.
- [16] J. Yang, Z. Shen, "A thin and broadband absorber using double-square loops," *IEEE Antennas Wirel. Propag. Lett.*, 6: 388-391, 2007.
- [17] S. Li, et al. "Wideband, thin, and polarization-insensitive perfect absorber based the double octagonal rings metamaterials and lumped resistances," *J. Appl. Phys.*, 116: 043710, 2014.
- [18] W. Tang, Z. Shen, "Simple design of thin and wideband circuit analogue absorber," *Electron. Lett.*, 43 (12): 689-691, 2007.
- [19] Y. Z. Cheng, et al., "Design, fabrication and measurement of a broadband polarization-insensitive metamaterial absorber based on lumped elements," *J. Appl. Phys.*, 111: 044902, 2012.
- [20] P. Munaga, et al. "A fractal-based compact broadband polarization insensitive metamaterial absorber using lumped resistors," *Microw. Opt. Technol. Lett.*, 58(2): 343-347, 2016.
- [21] Y. Shang, Z. Shen, S. Xiao, "On the design of single-layer circuit analog absorber using double-square-loop array," *IEEE Trans. Antennas Propag.* 61(12): 6022-6029, 2013.
- [22] Y. Han, W. Che, C. Christopoulos, Y. Xiong, Y. Chang, "A fast and efficient design method for circuit analog absorbers consisting of resistive square-loop arrays," *IEEE Trans. Electromagn. Compat.*, 58(3): 747-757, 2016.
- [23] M. A. Shukoor, S. Dey, "A novel modified circular ring-based broadband polarization-insensitive angular stable circuit analog absorber (CAA) for RCS applications," *Int. J. Microwave Wireless Technol.*, 15: 440-453, 2022.
- [24] C. Barde, et al. "Angle-independent wideband metamaterial microwave absorber for C and X band application," *Int. J. Microwave Wireless Technol.*, 16: 101-109, 2023.
- [25] A. A. G. Amer, et al., "A wide-angle, polarization-insensitive, wideband metamaterial absorber with lumped resistor loading for ISM band applications," *IEEE Access*, 12: 42629-42641, 2024.
- [26] Y. Zhang, et al., "Design and Analysis of a Broadband Microwave Metamaterial Absorber," *IEEE Photonics J.*, 15(3), 2023.
- [27] K. M. R. Islam, et al., "Design and experimental performance evaluation of a single-layer polarization-insensitive asymmetric microwave metasurface absorber," *IEEE Trans. Antennas Propagation.*, 72(8): 6520-6529, 2024.
- [28] M. Zhang, et al., "Design of wideband absorber based on dual-resistor-loaded metallic strips," *Int. J. Antennas Propag.*, 1238656: 1-8, 2020.
- [29] S. Ghosh, et al., "Design, characterization and fabrication of a broadband polarization insensitive multi-layer circuit analogue absorber," *IET Microwaves Antennas Propag.*, 10(8): 850-855, 2016.
- [30] J. Chen, Y. Shang, C. Liao, "Double-layer circuit analog absorbers based on resistor-loaded square-loop arrays," *IEEE Antennas Wirel. Propag. Lett.*, 17(4): 591-595, 2018.
- [31] P. Jain, et al., "Machine learning techniques for predicting metamaterial microwave absorption performance: A comparison," *IEEE Access*, 11: 128774-128783, 2023.
- [32] Y. Wei, et al., "A multiband, polarization-controlled metasurface absorber for electromagnetic energy harvesting and wireless power transfer," *IEEE Trans. Microwave Theory Tech.*, 70(5): 2861-2871, 2022.
- [33] R. M. H. Bilal, et al., "Polarization-controllable and angle-insensitive multiband Yagi-Uda-shaped metamaterial absorber in the microwave regime," *Opt. Mater. Express*, 12: 798-810, 2022.
- [34] J. Wang, et al., "Polarization-controlled and flexible single-/penta-band metamaterial absorber," *Materials*, 11: 1619, 2018.

Biographies



Saeedeh Barzegar-Parizi received the B.Sc. degree from the Iran University of Science and Technology, Tehran, Iran, in 2008, and the M.Sc. and Ph.D. degrees from the Sharif University of Technology, Tehran, in 2010 and 2015, respectively, all in electrical engineering. She has been with the Department of Electrical Engineering, Sirjan University of Technology, where she is currently an Associate Professor. Her research interests include the numerical and analytical solving of periodic structures, photonics designs/devices, plasmonics, metamaterials, optical and biomedical sensors, Microwave devices, Propagation.

- Email: barzegarparizi@sirjantech.ac.ir
- ORCID: [0000-0002-7467-7677](https://orcid.org/0000-0002-7467-7677)
- Web of Science Researcher ID: AAP-2310-2020
- Scopus Author ID: 36697630200
- Homepage: <https://sirjantech.ac.ir/%d8%b3%d8%b9%db%8c%d8%af%d9%87-%d8%a8%d8%b1%d8%b2%da%af%d8%b1-%d9%be%d8%a7%d8%b1%db%8c%d8%b2%db%8c/>

How to cite this paper:

S. Barzegar-Parizi, "Circuit analog absorber based on a double-layer of resistor-loaded strip arrays with various bandwidths according to selecting the polarization," *J. Electr. Comput. Eng. Innovations*, 13(2): 299-306, 2025.

DOI: [10.22061/jecei.2024.11244.781](https://doi.org/10.22061/jecei.2024.11244.781)

URL: https://jecei.sru.ac.ir/article_2239.html

